Critical immunosuppressive effect of MDSC-derived exosomes in the tumor microenvironment

MOHAMMAD H. RASHID[1,2], THAIZ F. BORIN[1], ROXAN ARA[1], RAZIYE PIRANLIOGLU[1], BHAGELU R. ACHYUT[3], HASAN KORKAYA[4], YUTAO LIU[5] and ALI S. ARBAB[1]

[1]Laboratory of Tumor Angiogenesis, Georgia Cancer Center, Department of Biochemistry and Molecular Biology, Augusta University, Augusta, GA 30912; [2]Nanomedicine Research Center, Department of Neurosurgery, Cedars-Sinai Medical Center, Los Angeles, CA 90048; [3]Cancer Animal Models Shared Resource, Winship Cancer Institute, Emory University, Atlanta, GA 30322; [4]Molecular Oncology and Biomarkers Program, Georgia Cancer Center, Department of Biochemistry and Molecular Biology, Augusta University; [5]Department of Cellular Biology and Anatomy, Medical College of Georgia, Augusta University, Augusta, GA 30912, USA

Received June 30, 2020; Accepted December 9, 2020

DOI: 10.3892/or.2021.7936

Abstract. Myeloid-derived suppressor cells (MDSCs) are an indispensable component of the tumor microenvironment (TME). Along with the role of MDSC immunosuppression and antitumor immunity, MDSCs facilitate tumor growth, differentiation, and metastasis in several ways that are yet to be explored. Like any other cell type, MDSCs also release a tremendous number of exosomes, or nanovesicles of endosomal origin, that participate in intercellular communications by dispatching biological macromolecules. There have been no investigational studies conducted to characterize the role of MDSC-derived exosomes (MDSC exo) in modulating the TME. In this study, we isolated MDSC exo and demonstrated that they carry a significant level of proteins that play an indispensable role in tumor growth, invasion, angiogenesis, and immunomodulation. We observed a higher yield and more substantial immunosuppressive potential of exosomes isolated from MDSCs in the primary tumor area than those in the spleen or bone marrow. Our *in vitro* data suggest that MDSC exo are capable of hyper-activating or exhausting CD8 T-cells and induce reactive oxygen species production that elicits activation-induced cell death. We confirmed the depletion of CD8 T-cells *in vivo* by treating mice with MDSC exo. We also observed a reduction in pro-inflammatory M1-macrophages in the spleen of those animals. Our results indicate that the immunosuppressive and tumor-promoting functions of MDSCs are also implemented by MDSC-derived exosomes which would open up a new avenue of MDSC research and MDSC-targeted therapy.

Correspondence to: Dr Ali S. Arbab, Laboratory of Tumor Angiogenesis, Georgia Cancer Center, Department of Biochemistry and Molecular Biology, Augusta University, 1410 Laney Walker Blvd., Room CN 3315, Augusta, GA 30912, USA
E-mail: aarbab@augusta.edu

Key words: exosomes, myeloid-derived suppressor cells, tumor microenvironment, CD8 T cells, activation-induced cell death

Introduction

Apart from cancer cells, the tumor microenvironment (TME) consists of heterogeneous host cells of the immune system, the tumor vasculature and lymphatics, fibroblasts, pericytes, and sometimes adipocytes (1). Myeloid-derived suppressor cells (MDSCs) are crucial components of the TME that play a pivotal role in tumor growth, neovascularization, and metastasis (2-4). MDSCs are a group of vastly heterogeneous immunosuppressive cells derived from immature myeloid progenitors that have been linked to poor patient prognosis (5). Typically, immature myeloid cells traverse to the peripheral organs after originating from bone marrow and rapidly mature into macrophages, dendritic cells, or granulocytes (neutrophils, eosinophils, and basophils) (6). That said, in the tumor condition, multifarious factors that are present in the TME prevent the differentiation of these immature myeloid cells and instigate their actuation into an immunosuppressive phenotype (7). MDSCs are usually divided into two subpopulations: gMDSCs (granulocytic, $CD11b^{+}Ly6G^{+}Ly6C^{low}$), which are identical to neutrophils, and mMDSCs (monocytic, $CD11b^{+}Ly6G^{-}Ly6C^{hi}$), which are consistent with monocytes with respect to morphology and phenotype (8,9).

There is growing evidence that MDSCs harness various immune and nonimmune mechanisms to promote tumor development. MDSCs inhibit adaptive antitumor immunity by inhibiting T-cell activation and function (T-cell receptor down-regulation, T-cell cell cycle inhibition, and immune checkpoint blockade) (9), and by driving and recruiting T regulatory cells. Immunosuppression by MDSCs is also mediated by the generation of reactive oxygen species (ROS) (10) and cytokine release [interleukin (IL)-10 and tumor growth factor (TGF)-β] (11,12), in conjunction with arginine depletion (13). They inhibit innate immunity by polarizing macrophages toward a type 2

tumor-promoting phenotype (M2-macrophage) (14) and by inhibiting natural killer (NK) cell-mediated cytotoxicity (15). Likewise, MDSCs are efficient recruiters of other immunosuppressive cells.

Although the role of MDSCs in tumor growth and metastasis is well known, there is a significant knowledge gap for understanding the role of MDSC-derived exosomes (MDSC exo). During the past decade, there has been a huge surge of exosome research and publications that are mostly focused on exosomes derived from tumor cells and immune cells. Exosomes are 30-150 nm lipid bi-layered extracellular bioactive vesicles of endosomal origin that are secreted by all cells and are present in various body fluids. Exosomes have been proposed to act as intercellular communicators as they can transfer their cargo (proteins, lipids, and nucleic acids) to nearby or distant recipient cells. Previously, we observed that MDSC exo carry a significant amount of pro-tumorigenic factors, and a large percentage of MDSC exo injected intravenously was found to be distributed in the primary breast tumor and metastatic sites (16). These findings warrant us to further explore the implication of MDSC exo in immunosuppression and tumor progression mechanisms.

In this study, we characterized the size, yield, and contents of exosomes collected from different MDSC populations and immature myeloid progenitor cells. We now report that, similar to parental MDSCs, exosomes from MDSCs also play a crucial role in inciting the immunosuppressive milieu by way of limiting the functions of cytotoxic T cells and pro-inflammatory M1 macrophages in the TME.

Materials and methods

Ethics statement. All experiments were performed according to the National Institutes of Health (NIH) guidelines and regulations. The Institutional Animal Care and Use Committee (IACUC) of Augusta University (protocol #2014-0625) approved the experimental procedures. All animals were kept under regular barrier conditions at room temperature with exposure to light for 12 h and dark for 12 h. Food and water were offered *ad libitum*. All efforts were made to ameliorate the suffering of animals. CO_2 with a displacement rate of 30-70% of the cage volume and delivery rate of two liters/min into the cage followed by a secondary method was used to euthanize animals for tissue collection.

Nanoparticle tracking analysis. Nanoparticle tracking analysis (NTA) was performed using ZetaView, a second-generation instrument from Particle Metrix for visualizing and counting individual exosome particles as described previously (16,17). This high-performance integrated instrument is equipped with a cell channel that is integrated into a 'slide-in' cassette and a 405-nm laser. Samples were diluted between 1:100 and 1:2,000 in PBS and injected in the sample chamber with sterile syringes (BD Discardit II). Ten microliters of EXO suspension was loaded into the sample chamber and all measurements were performed at 23˚C and pH 7.4. We used 11 positions with 2 cycles for the measurement mode, and a maximum pixel of 200 and minimum of 5 for the analysis parameters. ZetaView 8.02.31 software and Camera 0.703 μm/px were used for capturing and analyzing the data.

Flow cytometry. For the *in vivo* flow cytometric analysis, the collected fresh tissue was dispersed into single cells by filtering through a 70-μm cell strainer, and spun at 1,200 rpm for 15 min. For the *in vitro* flow cytometric analysis, cells were washed twice with sterile PBS. The pellet was re-suspended in 1% BSA/PBS and incubated with LEAF blocker (Stem Cell Technologies, cat. #19867) in 100 μl volume for 15 min on ice to reduce non-specific staining. The single cells were then labeled to detect the immune cell populations using fluorescence conjugated antibodies for CD3 (cat. #100204), CD4 (cat. #100512), CD8 (cat. #100732), CD206 (cat. #141708), F4/80 (cat. #123116), CD279 (cat. #135208 and 124312), CD25 (cat. #101910), CD184 (cat. #146506), CD194 (cat. #131204), CD69 (cat. #104506), CD62L (cat. #104432), CD11b (cat. #101208 and 101228), CD80 (cat. #1047220), CD86 (cat. #105028), Gr1 (cat. #108406), Ly6C (cat. #128012), Ly6G (cat. #127614), and CD45 (cat. #103108). All antibodies were mouse-specific (BioLegend), and the samples were acquired using the Accuri C6 flow cytometer (BD Biosciences). A minimum of 50,000 events were acquired.

Tumor model. Both 4T1 and AT3 cells expressing the luciferase gene were orthotopically implanted in syngeneic BALB/c and C57BL/J6 mice, respectively (The Jackson Laboratory, Bar Harbor, Maine, USA). All mice were between 5-6 weeks of age and weighed 18-20 g. Animals were anesthetized using a mixture of xylazine (20 mg/kg) and ketamine (100 mg/kg) administered intraperitoneally. Hair was removed from the right half of the abdomen using hair removal ointment, and then the abdomen was cleaned by povidone-iodine and alcohol. A small incision was made in the middle of the abdomen, and the skin was separated from the peritoneum using blunt forceps. The separated skin was pulled to the right side to expose the mammary fat pad and either 50,000 4T1 cells or 100,000 AT3 cells in 50 μl Matrigel (Corning Inc.) were injected.

Isolation of MDSCs. MDSCs were isolated from spleens and tumors of tumor-bearing mice 3 weeks after orthotopic tumor cell implantation. Myeloid progenitor cells were isolated from the bone marrow of normal wild-type mice. We used anti-mouse Ly-6G, and Ly-6C antibody-conjugated magnetic beads (BD Biosciences). The purity of cell populations was >99%. In short, the spleen was disrupted in PBS using the plunger of a 3 ml syringe, and cell aggregates and debris were removed by passing the cell suspension through a sterile 70-μm mesh nylon strainer (Fisherbrand™). Mononuclear cells were separated by lymphocyte separation medium (Corning®) as a white buffy coat layer. Cells were then centrifuged at 1,500 rpm for 10 min followed by a washing step with PBS at 1,200 rpm for 8 min. Then cells were resuspended at $1x10^8$ cells/ml in PBS and antibodies conjugated with magnetic beads were added followed by incubation at 4˚C for 30 min. Finally, positive cells were collected using a MACS LS column (Miltenyi Biotec) and a MidiMACS™ magnetic stand followed by a wash step with extra PBS. The purity of isolated MDSCs was checked by flow cytometry using Gr1 FITC and CD11b APC antibodies (purchased from BioLegend). Cell viability was checked with 7-AAD which was less than 0.1-0.2% (dead cells) of the total population. MDSCs were grown in exosome-depleted media consisting of RPMI, 2 mM L-glutamine, 1% MEM

non-essential amino acids, 1 mM sodium pyruvate, and 10% FBS, supplemented with 100 ng/ml of GM-CSF.

Exosome isolation. Exosomes were depleted from the complete media by ultracentrifugation for 70 min at 100,000 x g using an ultracentrifuge (Beckman Coulter) and SW28 swinging-bucket rotor. MDSCs ($6x10^6$) were grown in a T175 flask for 72 h under normoxic conditions (5% CO_2 and 20% oxygen) at 37˚C in a humidified incubator. The cell culture supernatant was centrifuged at 700 x g for 15 min to remove cell debris. To isolate exosomes, we employed a combination of two steps of the size-based method by passing through a 0.20-μm syringe filter and centrifugation with 100k membrane tube at 3,200 x g for 30 min followed by a single step of ultracentrifugation at 100,000 x g for 70 min [as described in our previous publication (16)].

Protein quantification. Isolated exosomes resuspended in a minimal amount of PBS were lysed by RIPA buffer with protease and phosphatase inhibitor (100:1 dilution). Exosomal protein was quantified by Bradford assay using Pierce™ BCA Protein Assay Kit (Thermo Scientific™) and serial dilution of BSA standard (Thermo Scientific™; Thermo Fisher Scientific, Inc.).

Protein array. Proteins were extracted from tumor cells and their corresponding exosomes in both untreated and treated conditions to evaluate the expression profiles of 44 factors in duplicate by mouse cytokine antibody array (AAM-CYT-1000-8; RayBiotech, Inc.). Protein sample (500 μg) was loaded onto the membrane according to the manufacturer's instructions, and the chemiluminescent reaction was detected using a LAS-3000 imaging system (Fuji Film, Japan). All signals (expression intensity) emitted from the membrane were normalized to the average of 6 positive control spots of the corresponding membrane using ImageJ software version 1.53c [National Institutes of Health (NIH)].

In vitro migration assay. A Transwell assay was performed to evaluate the chemotaxis property of the MDSC-derived exosomes. We used 24 Transwell plates with 8-μm inserts in polyethylene terephthalate track-etched membranes (Corning, Inc.). We collected bone marrow cells and splenic mononuclear cells using Ficoll gradient centrifugation, and myeloid cells from bone marrow using $CD11b^+$ magnetic beads from normal Balb/c mice. A total of $1.5x10^6$ cells/insert in serum-free media were added into the upper compartment of the chamber. Inserts were placed in 12-well plates with DMEM containing 0.5% FBS in the presence or absence of exosomes (20 μl containing approximately $3x10^8$ exosomes) isolated from MDSCs. After incubating overnight, we collected suspended immune cells (migrated) from the media of the bottom chamber and loosely adherent immune cells on the surface of the bottom chamber using gentle cell scraping. Then we centrifuged and resuspended the cells in PBS and counted the cells with a hemocytometer. Insert membranes were washed, fixed, and stained with 0.05% crystal violet to detect the migrated/invaded cells. The counting was made with an inverted microscope (Nikon Eclipse E200).

In vitro scratch assay. Scratch assay was performed to detect the ability of MDSC-derived exosomes to increase migration and invasion of tumor cells. 4T1 luciferase positive cells were seeded in 6-well plates. After achieving 80-90% confluency, the cells were starved overnight with 0.5% FBS for cell cycle synchronization and a measured wound was inflicted at the center of the culture (from top to bottom). Then, cells were treated with 50 μl of splenic MDSC-derived exosomes in PBS containing $7.5x10^8$ exosomes for 48 h in 2% FBS media. Microphotographs were taken every 24 h using an automated all-in-one microscope (BZ-X710; Keyence). The wound size was measured using Image J software (NIH) by drawing a rectangular region of interest to quantify the visible area of the wound.

In vivo treatment with MDSC-derived exosomes. MDSC-derived exosomes were injected intravenously (100 μl containing approximately $1.5x10^9$ exosomes) into the wild-type Balb/c and C57Bl/6 mice. The animals were treated for a week with 3 doses (alternate days) of MDSC-derived exosomes. After that, the animals were euthanized and organs were collected for flow cytometric analysis.

Isolation of T cells. Both $CD4^+$ and $CD8^+$ cells were isolated from normal mouse splenocytes by immune-magnetic negative selection kit (Stemcell Technology; catalog #19852 and 19853, respectively). In short, harvested spleens from normal mice were disrupted in cold PBS containing 2% FBS. Clumps and debris were removed by passing the cell suspension through a 70-μm mesh nylon strainer. The single-cell suspension was centrifuged at 300 x g for 10 min and resuspended at $1x10^8$ nucleated cells/ml. Rat serum was added to the sample (50 μl/ml) followed by the addition of isolation cocktail (50 μl/ml). After mixing, the sample mix was incubated at room temperature for 10 min. RapidSpheres™ (75 μl/ml) were added to the sample mix and incubated for 3 min. The tube was placed in EASYSEP™ MAGNETS (catalog #18001; Stemcell Technologies) for 3 min. The enriched cell suspension was collected by decanting into a new tube. Cells were seeded in 24-well plates bound with purified anti-mouse CD3e (5 μl/ml) in T-cell media that consists of RPMI, 10% FBS, 1% MEAM, 2.5% HEPES, 1% penicillin-streptomycin, 0.5% β-mercaptoethanol, and purified anti-mouse CD28 (5 μl/ml).

Quantification of ROS generation by $CD8^+$ T-cells. ROS production from $CD8^+$ T-cells following MDSC-derived exosomes treatment *in vitro* was estimated by labeling the $CD8^+$ T-cells using CM-H_2DCFDA (Invitrogen™, C6827; Thermo Fisher Scientific, Inc.). In short $CD8^+$ T-cells were isolated according to the above-mentioned method. After the final wash step of the isolation procedure, cells were resuspended in 1 ml PBS. DCFDA solution at a working concentration of 10 μM/ml was added followed by incubation in the dark at 37˚C for 30 min. The cells were washed with an extra PBS to remove the unbound dye and resuspended with appropriate T-cell media. A total of 100,000 cells were seeded per well of 96 well-plate. MDSC-derived exosomes were added in the treatment group and the same volume of PBS was added in the control group. Hydrogen peroxide (H_2O_2) was used as a positive control for ROS production. Following 4 h of incubation,

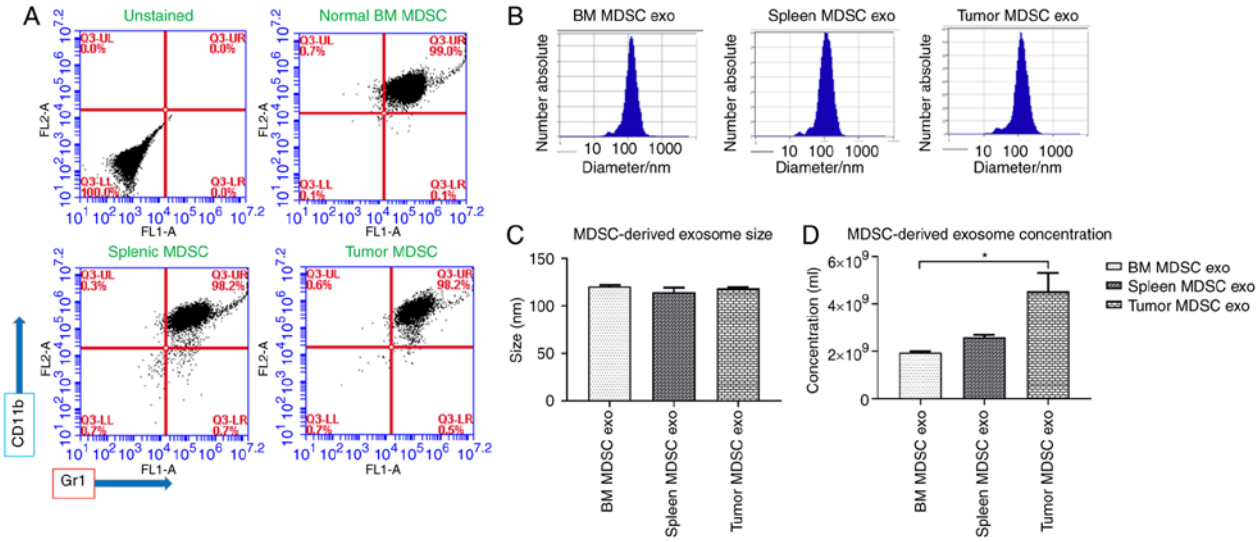

Figure 1. Isolation of MDSC-derived exosomes (exo) from different sources. (A) Flow cytometric analysis of isolated MDSCs from normal bone marrow (BM), spleen of tumor-bearing mice, and tumors, showing that more than 98% of cells were positive for CD11b and Gr1. (B and C) Nanoparticle tracking analysis (NTA) showing no significant differences in the size distribution of exosomes isolated from MDSCs of normal bone marrow (BM), the spleen of tumor-bearing mice, and tumors. (D) NTA analysis showing exosome concentration per ml. Quantitative data are expressed in mean ± SEM. *P<0.05. n=3. MDSCs, myeloid-derived suppressor cells.

the fluorescent intensity of each condition was measured using a Perkin Elmer Victor3 V 1420 multilabel plate reader (PerkinElmer), with excitation and emission wavelengths of 485 and 535 nm, respectively. Each condition was assayed in triplicate for significance.

$CD8^+$ T-cell proliferation assay. Following isolation, 20,000 $CD8^+$ cells were seeded in an anti-mouse CD3e-bound 96-well plate and treated with 10 μl of MDSC-derived exosomes or the same volume of PBS (control). After 48 h, 10 μl of WST-1 reagent (Alkali Scientific Inc.) was added to each well and incubated for 4 h. The absorbance of each well was measured at a wavelength of 450 nm by the Perkin Elmer Victor3 V 1420 multilabel plate reader.

Statistical analysis. Quantitative data are expressed as mean ± standard error of the mean (SEM) unless otherwise stated, and statistical differences between more than two groups were determined by analysis of variance (ANOVA) followed by multiple comparisons using Tukey's multiple comparisons test. A comparison between 2 samples was performed by the Student t-test. GraphPad Prism version 8.2.1 for Windows (GraphPad Software, Inc.) was used to perform the statistical analysis. Differences with P-values <0.05 were considered significant and are indicated in the figures and legends (*P<0.05, **P<0.01, ***P<0.001, ****P<0.0001).

Results

Isolation and characterization of exosomes from different MDSC populations. We isolated MDSCs from the bone marrow of normal (non-tumor bearing) wild-type mice, and from spleen and tumors of tumor-bearing mice by magnetic particle separation using Ly6G and Ly6C beads. Tumors were implanted orthotopically in the mammary fat pad and allowed to grow for 3 weeks. Following their separation, by flow cytometry, more than 98% of the cells were estimated to be positive for MDSC markers ($CD11b^+Gr^+$) (Fig. 1A). Cell viability was checked with 7-AAD and determined to be less than 0.1-0.2% of the total population (Fig. S1). After 72 h, we isolated exosomes from culture supernatant and characterized them by NTA. Exosomes isolated from MDSCs of normal bone marrow (BM MDSC exo), the spleen of tumor-bearing mice (spleen MDSC exo), and tumors (tumor MDSC exo) were similar in size and distribution (Fig. 1B and C). However, MDSCs from tumors released significantly more exosomes compared to MDSCs from normal bone-marrow, which could be due to the presence of the stressful condition, and more active and immunosuppressive MDSCs in the primary tumor area (Fig. 1D).

Next, we tested if the protein contents of normal BM MDSC exo differ from the spleen MDSC exo and tumor MDSC exo isolated from tumor-bearing mice. We quantified the expression level of cytokines in MDSC exo that are involved in tumor invasion (Fig. 2A), myeloid cell activation and function (Fig. 2B), and angiogenesis (Fig. 2C) by membrane-based protein array. All the cytokines were significantly overexpressed in exosomes isolated from MDSCs of tumor-bearing mice (in both spleen MDSC exo and tumor MDSC exo) compared to normal BM MDSC exo. Interestingly, tumor MDSC exo showed a higher level of expression than that of spleen MDSC exo indicating that MDSC-derived exosomal cytokine contents are different based on the microenvironment of the host tissues.

MDSC-derived exosomes promote invasion and migration of tumor cells. MDSCs were demonstrated to promote tumor invasion and metastasis by two mechanisms: i) Increased production of multiple matrix metalloproteinases (MMPs) for extracellular matrix degradation and increased production of chemokines to establish a pre-metastatic milieu (18,19), and ii) merging with tumor cells, thus promoting the metastatic process (20,21). We observed significantly higher expression of invasion and migration-associated cytokines in the spleen

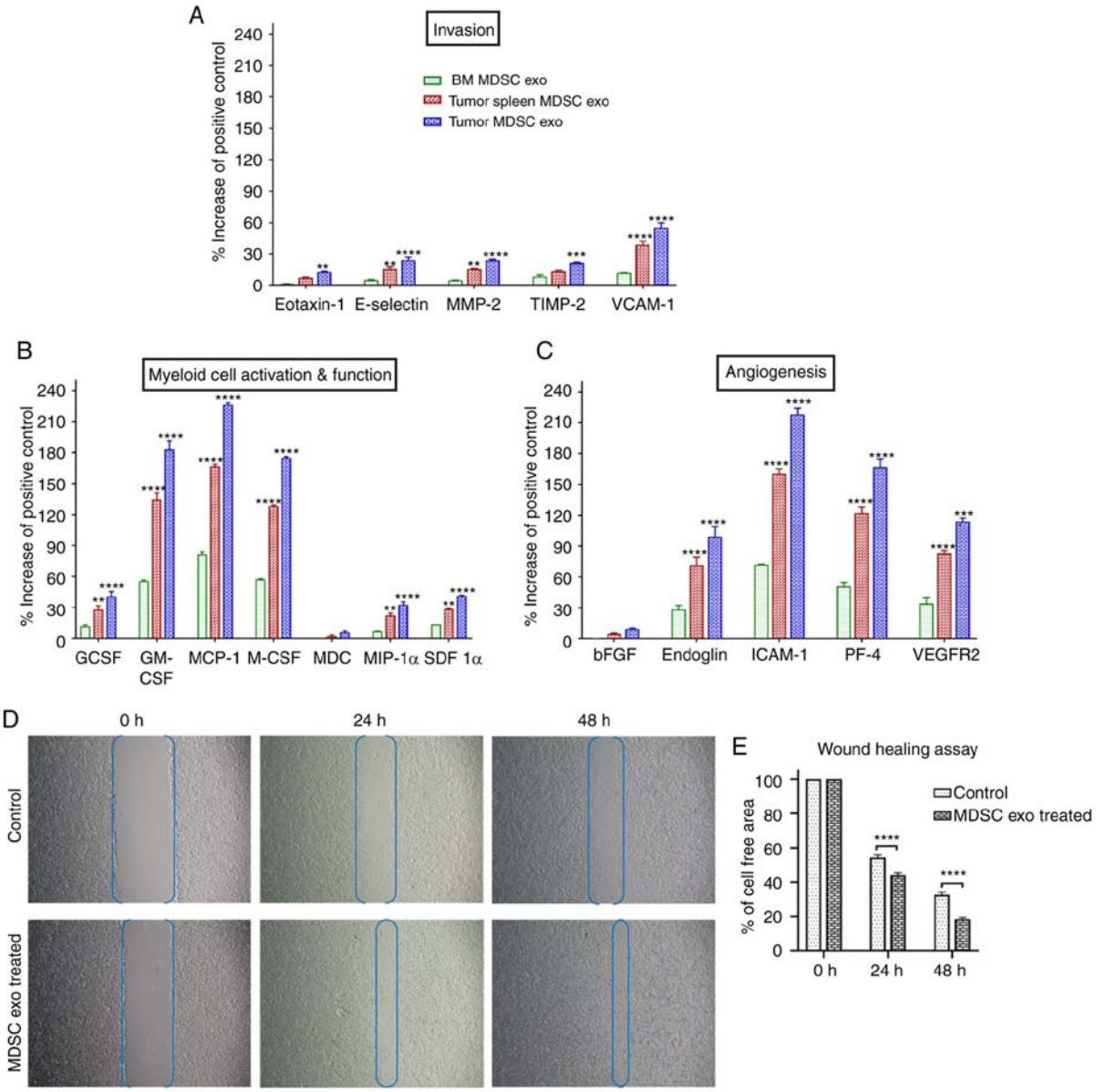

Figure 2. The expression level of cytokines in MDSC-derived exosomes (exo) that are involved in tumor invasion, angiogenesis, and myeloid cell activation and function. *In vitro* quantification of the level of cytokines associated with (A) tumor invasion, (B) myeloid cell activation and function, and (C) angiogenesis, detected in the membrane-based array in protein samples collected from exosomes isolated from MDSCs of normal bone marrow (BM), the spleen of tumor-bearing mice and tumors. Quantitative data are expressed as mean ± SEM. **P<0.01, ***P<0.001, ****P<0.0001, compared to the BM MDSC exo. n=4. (D and E) The role of MDSC-derived exosomes in tumor cell migration was evaluated by a wound-healing assay/scratch assay, carried out in the 4T1 murine breast cancer cell line with or without (control) splenic MDSC-derived exosome treatment. (D) Representative microscopic images (x4 magnification) are shown before treatment, and 24 and 48 h after treatment. (E) Semi-quantitative analysis of the percentage of non-covered area/cell-free area. Quantitative data are expressed as mean ± SEM. ****P<0.0001. n=10. MDSCs, myeloid-derived suppressor cells; MMP-2, Matrix metalloproteinase-9; TIMP-2, tissue inhibitor of metalloproteinase 2; VCAM-1, vascular cell adhesion molecule 1; GCSF, granulocyte colony-stimulating factor; GM-CSF, granulocyte/macrophage colony stimulating factor; MCP-1, monocyte chemoattractant protein-1; M-CSF, macrophage colony-stimulating factor; MDC, macrophage-derived chemokine; MIP-1α, macrophage inflammatory protein-1α; SDF 1α, stromal cell-derived factor 1α; bFGF, basic fibroblast growth factor; ICAM-1, intercellular adhesion molecule-1; PF-4, platelet factor 4; VEGFR2, vascular endothelial growth factor receptor 2.

MDSC-exo of tumor-bearing mice compared to normal BM MDSC-exo, which led us to further investigate the role of MDSC exo in promoting invasion and migration of tumor cells. *In vitro*, the wound-healing assay showed a significantly increased migration of 4T1 tumor cells in the spleen of the MDSC-exo treated group compared to the untreated control group at 24 and 48 h (Fig. 2D and E).

MDSC exosomes promote the recruitment of immunosuppressive cells in vitro. Tumor-specific endocrine factors systemically stimulate the quiescent immune-compartments (bone marrow, spleen, lymph nodes), resulting in the expansion, mobilization, and recruitment of immunosuppressive cells. Discrete subsets of tumor-instigated immune cells bolster tumor progression and metastasis by governing angiogenesis, inflammation, and immune suppression. Of the immune cells, much focus has been denoted towards the MDSCs (22), tumor-associated macrophages (TAMs) (23), Tie2-expressing monocytes (24), vascular endothelial (VE)-cadherin^{+}CD45^{+} vascular leukocytes, and infiltrating mast cells and

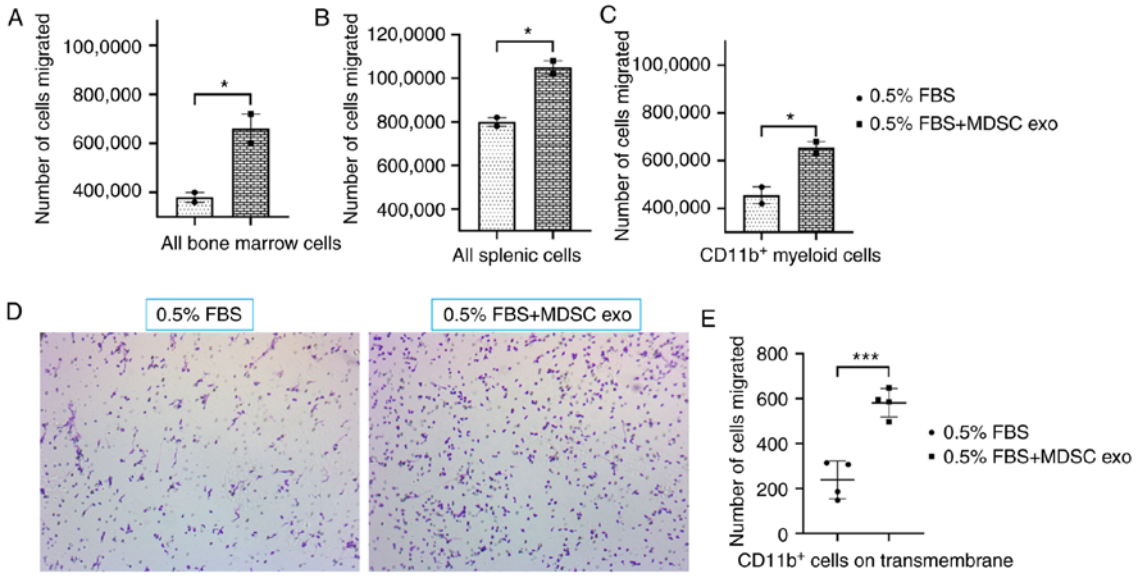

Figure 3. Role of MDSC-derived exosomes (exo) in immune cell migration. Isolated mouse myeloid cells, bone marrow cells, and splenic cells were seeded on the top chamber of the Transwell, and splenic MDSC-derived exosomes were added in the bottom chamber with 0.5% FBS. After 24 h, migrated (A) bone marrow cells, (B) splenic cells, and (C) myeloid cells in the bottom chamber were counted with a hemocytometer. In addition, (D) attached myeloid cells on the Transwell membrane were visualized under a light microscope, and (E) quantified. Quantitative data are expressed as mean ± SEM. *P<0.05, ***P<0.001, n=4. MDSCs, myeloid-derived suppressor cells.

neutrophils (25,26). We observed significant high expression levels of cytokines crucial for immunosuppressive cell mobilization and recruitment in spleen MDSC-exo isolated from splenic MDSCs of tumor-bearing mice compared to normal BM MDSC exo.

To determine the chemotaxis capability of MDSC exo, we seeded CD11b^{+} myeloid cells (from bone marrow) or all bone marrow cells, or all splenic mononuclear cells (following Ficoll separation) isolated from normal mice in the upper chamber and with or without spleen MDSC exo in the bottom chamber of the Transwell insert. After 24 h of incubation, the number of migrated cells in the bottom chamber was significantly higher in the wells treated with spleen MDSC exo compared to untreated control wells (Fig. 3A-C). We also washed, fixed, and stained the insert membranes (of the CD11b^{+} cell-incubated group) with 0.05% crystal violet to detect the migrated/invaded cells. The number of cells that attached to the membrane were visualized by microscopy (Fig. 3D) and later quantified by an ImageJ cell counter. A significantly higher number of CD11b^{+} myeloid cells were attached to the transmembrane in the wells treated with spleen MDSC exo compared to the untreated control wells (Fig. 3E).

Expression of T-cell function-associated and immunomodulatory cytokines in exosomes from different MDSC populations. We further estimated the level of expression of T-cell function-associated and immunomodulatory cytokines in the protein contents of normal BM MDSC exo and exosomes isolated from MDSCs (tumor and splenic) of tumor-bearing mice by protein array. Among the immunomodulatory cytokines, the levels of IL-12, IL-13, IL-1Ra, IL-4, C-X-C motif chemokine 5 (LIX), and tumor necrosis factor (TNF)-α were significantly elevated in both the tumor-MDSC-exo and spleen-MDSC-exo of tumor-bearing mice compared to normal BM-MDSC-exo (Fig. 4A). Among T-cell function-associated cytokines, IL-2, IL-7, L-selectin, and thymic stromal lymphopoietin (TSLP) were significantly higher in the exosomes derived both from the tumor and splenic MDSCs of tumor-bearing mice compared to normal BM MDSC-exo (Fig. 4B).

In vivo effect of MDSC-derived exosomes on T-cells. Next, we investigated whether MDSC exo treatment could deplete the CD8^{+} T-cells in mice. For this *in vivo* study, we used both C57BL/6 and Balb/c normal mice. We treated the mice with MDSC exo by intravenous (i.v.) injection through the tail vein for a week (total of 3 doses, alternate days). Then we euthanized the animals and harvested spleens for flow cytometric evaluation. The CD8^{+} T-cell population in splenic MDSC-exo treated animals was significantly declined compared to the untreated control group in both animal models (Fig. 5A and B). However, we did not observe any significant change in the CD4^{+} T-cell population.

In vivo effect of MDSC-derived exosomes on myeloid cells. We also explored whether the MDSC exo treatment could change the distribution of the myeloid populations *in vivo*. We noticed a significant reduction in M1-macrophages (CD11b^{+}CD80^{+} and CD11b^{+}CD86^{+}) and a notable increase of M2-macrophages (CD11b^{+}CD206^{+}) in the spleen of animals treated with spleen MDSC exo while we did not see a similar effect in the other organs (Fig. 6A). Representative dot-plots are provided in Figs. S2 and S3. There was a considerable decline in the monocytic MDSCs (CD11b^{+}Gr1^{+}Ly6C^{+}) and the expansion of granulocytic MDSCs (CD11b^{+}Gr1^{+}Ly6G^{+}) in the spleen of the treated animals compared to the untreated group (Fig. 6B). Representative dot-plots are provided in Fig. S4.

In vitro effect of MDSC-derived exosomes on T-cells. Since we demonstrated that MDSC exo express a significantly high

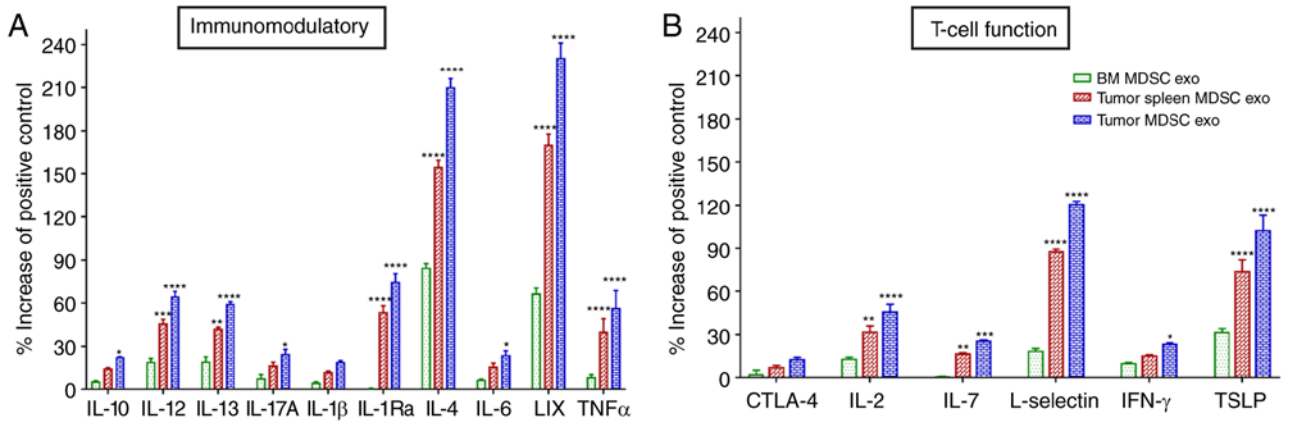

Figure 4. Expression levels of cytokines in MDSC-derived exosomes (exo) that are involved in T-cell function and immunomodulation. *In vitro* quantification of the level of cytokines associated with (A) immunomodulation and (B) T-cell function, detected in the membrane-based array in protein samples collected from the exosomes isolated from MDSCs of normal bone marrow (BM), the spleen of tumor-bearing mice and tumors. Quantitative data are expressed as mean ± SEM. *P<0.05, **P<0.01, ***P<0.001, ****P<0.0001, compared with the BM MDSC exo. n=4. MDSCs, myeloid-derived suppressor cells; IL, interleukin; LIX, C-X-C motif chemokine 5; TNFα, tumor necrosis factor α; CTLA-4, cytotoxic T-lymphocyte-associated protein 4; IFN-γ, interferon-γ; TSLP, thymic stromal lymphopoietin.

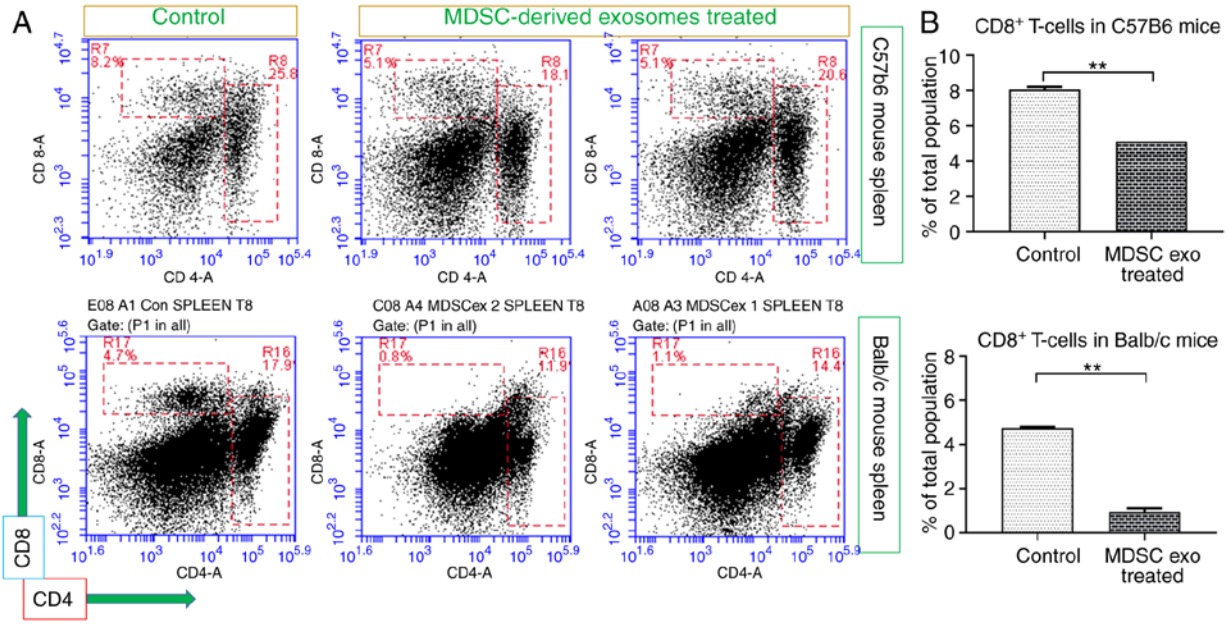

Figure 5. *In vivo* depletion of CD8^{+} T-cells by MDSC-derived exosome treatment. Normal Balb/c and C57BL/6 mice were treated with splenic MDSC-derived exosomes (exo) for 1 week and without treatment (control). (A) Representative flow cytometric plots and (B) quantification of cells from the spleen showed decreased number of CD8^{+} T-cells. Quantitative data are expressed as mean ± SEM. **P<0.01, n=4. MDSCs, myeloid-derived suppressor cells.

level of cytokines that facilitate regulatory T-cell or Th2 cell functions and immunosuppression, we wanted to investigate the effect of MDSC exo directly on CD4^{+} and CD8^{+} T-cells *in vitro*. We isolated both types of cells and treated them with spleen MDSC exo or with the same volume of PBS (control). After 24 h, we collected the cells and analyzed the functional marker changes by flow cytometry. Splenic MDSC exo-treated CD4^{+} T-cells expressed a significantly higher level of T-regulatory cell marker (CD25) and Th2 cell marker (CD184) compared to the control group (Fig. 7A). There was no change in the level of T-cell activation or exhaustion marker (CD279/PD-1). For the CD8^{+} T-cells, MDSC exo-treated cells showed a significantly higher level of T-cell activation marker (CD44), naïve T-cell marker (CD62L), and exhaustion marker (CD279) (Fig. 7B). Representative dot-plots are provided in the supplementary file (Figs. S5 and S6).

In vitro effect of MDSC-derived exosomes on CD8^{+} T-cell function and proliferation. MDSCs release ROS molecules as part of a primary mechanism to suppress T-cell responses (27). Considering the previous results on CD8^{+} T-cells, we further determined the level of ROS production by CD8^{+} T-cells after splenic MDSC exo treatment and also whether the treatment affects CD8^{+} T-cell proliferation. We labeled the CD8^{+} T-cells with CM-H_2DCFDA ROS probe and treated them with MDSC exo or with PBS (control). After 4 h, MDSC exo-treated CD8^{+} T-cells showed a considerably higher level of ROS production compared to the control (Fig. 7C). Although the cell

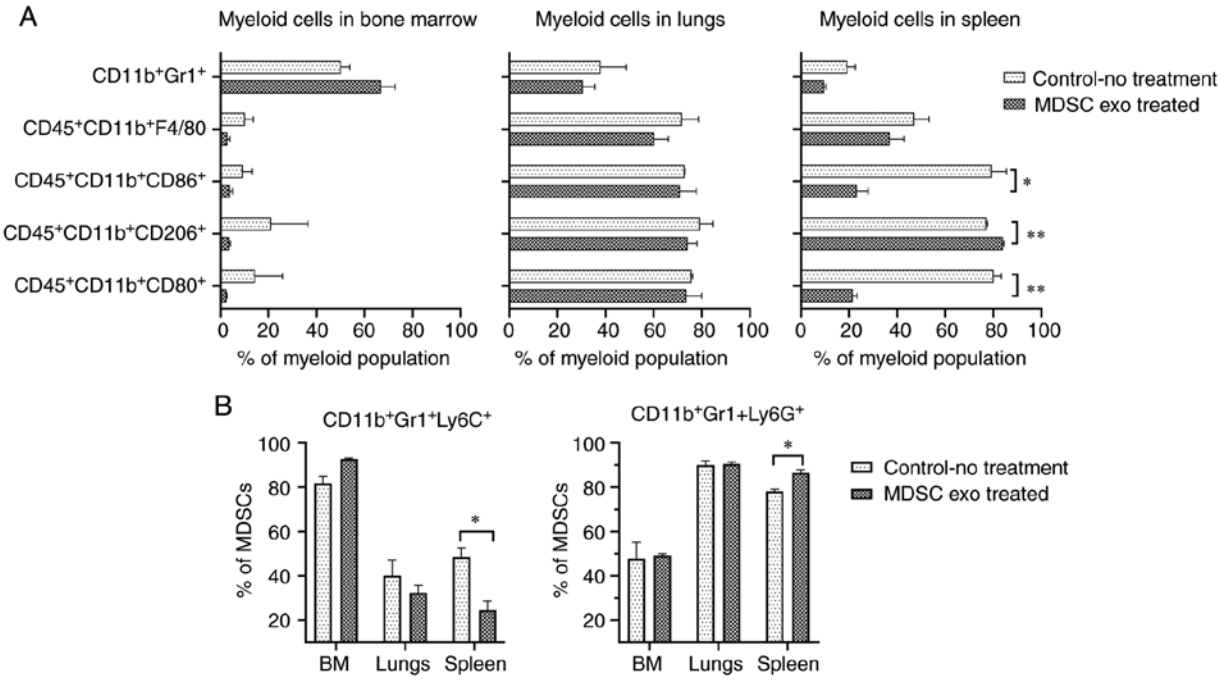

Figure 6. *In vivo* depletion of M1-macrophages, and increased number of M2-macrophages and gMDSCs by MDSC-derived exosome treatment. Normal Balb/c mice were treated with and without (control) splenic MDSC-derived exosomes for 1 week. Quantification of cells from the bone marrow (BM), lungs, and spleen showing (A) decreased number of M1-macrophages and increased M2-macrophages in the spleen and (B) decreased number of monocytic mMDSCs and increased number of granulocytic gMDSCs in the spleen following treatment with MDSC-derived exosomes. Quantitative data are expressed as mean ± SEM. *P<0.05, **P<0.01, n=4. MDSCs, myeloid-derived suppressor cells.

proliferation assay using WST-1 reagent showed a decreased number of $CD8^+$ T-cells in the MDSC exo group compared to the control group, it was not statistically significant (Fig. 7D).

Considering the fact that MDSC exo were able to activate and deplete $CD8^+$ T-cells, we determined the level of FasL in different MDSC exo that could conceivably trigger the apoptosis process in $CD8^+$ T-cells. We detected higher expression of FasL in the exosomes isolated from the MDSCs in tumors compared to that in exosomes of MDSCs from spleen and bone marrow (Fig. 7E). Furthermore, we quantified the activation markers of $CD8^+$ T-cells with or without treatment with MDSC exo by protein array. Treatment with MDSC exo appreciably increased the level of interferon (IFN)-γ while no significant changes in granzyme B and TNF-α level were observed (Fig. 7F).

Discussion

It has been perceived that functional differences may exist in myeloid-derived suppressor cells (MDSCs) isolated from different environments within the same host, and that MDSCs from tumors have a stronger immunosuppressive capacity than MDSCs in the peripheral lymphoid organs (spleen, lymph nodes) (28). We observed that exosomes were secreted more abundantly from tumor MDSCs, presumably due to the fact that MDSCs in the tumor microenvironment (TME) are in a more distressing milieu (e.g., hypoxia and acidic pH). It has been contemplated that cells may exploit exosome secretion to survive under stressful conditions (29-31). We also observed a higher concentration of proteins that are crucial for tumor growth, invasion, angiogenesis, and immunomodulation in exosomes isolated from MDSCs in tumors than those from the spleen or bone marrow. Although Haverkamp *et al* reported that MDSCs from inflammatory sites or tumor tissue possess the immediate ability to hamper T-cell function whereas those isolated from peripheral tissues were not suppressive without activation of iNOS by exposure to IFN-γ (32), we observed equivalent competency in MDSC exosomes (exo) isolated both from the tumor and spleen. However splenic MDSC exo demonstrated that to a lesser extent. For comparison as a control group, we used MDSCs from the bone marrow of normal wild-type animals. Although initially we wanted to use MDSCs from the spleen of normal/wild-type mice, it was quite impossible to isolate enough MDSCs from multiple spleens of wild-type animals while they were abundantly present in the spleen of tumor-bearing animals. Since distribution of MDSCs is very low (~1-2%) in normal spleen (8,33), we chose to use exosomes collected from bone marrow-derived MDSC as the control group. In spite of the fact that tumor MDSC exo had higher immunosuppressive potential, we used splenic MDSC exo (spleens were collected from tumor-bearing animals) for the downstream functional assays. Part of the reason was that MDSCs in the tumor-bearing mouse spleen were abundant for purification and growth in culture for adequate exosome isolation. Compared to the spleen, the number of MDSCs in the tumor was limited and we needed to pool MDSCs from multiple tumors to obtain enough cells for culture.

MDSCs are competent in promoting tumor growth through remodeling the TME (21,34). However, MDSCs are a miscellaneous population of immature myeloid cells that is comprised of monocytic and granulocytic subpopulations both of which have been shown to be immunosuppressive (35). It has been recently reported that early expansion and infiltration

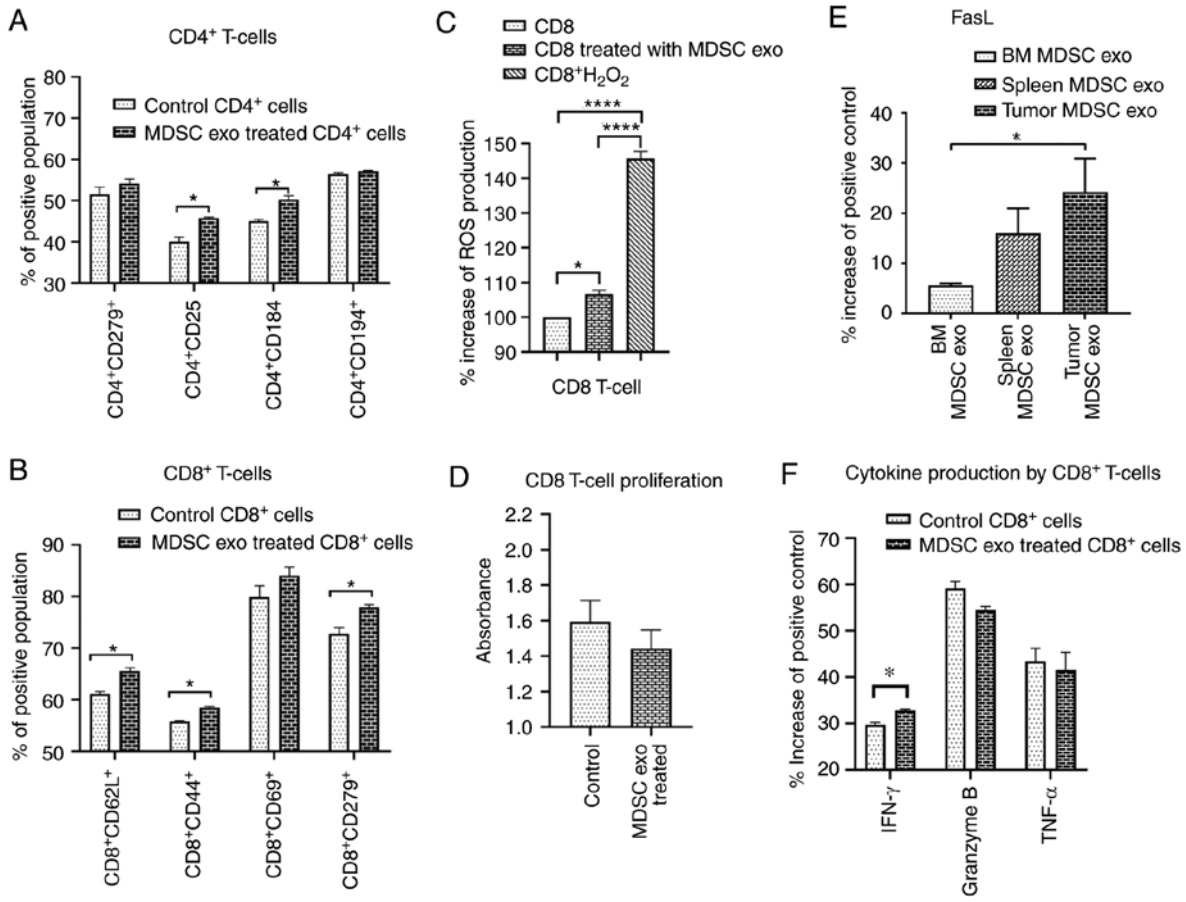

Figure 7. Effect of MDSC-derived exosomes on CD4 and CD8-positive T-cells *in vitro*. (A and B) Isolated CD4 and CD8-positive T-cells were co-cultured with or without splenic MDSC-derived exosome (exo) treatment for 24 h followed by flow cytometric analysis of the cells. (C) Effect of splenic MDSC-derived exosomes on ROS production by CD8+ T-cells was determined by CM-H_2DCFDA-labeled CD8+ T-cells treated with MDSC-derived exosomes. (D) Effect of splenic MDSC-derived exosomes on CD8+ T-cell proliferation by a cell proliferation assay using WST-1 reagent. (E and F) Membrane-based protein array was used to determine the (E) level of FasL in exosomes from different MDSC populations and (F) expression levels of cytokines in CD8 T-cells. Quantitative data are expressed as mean ± SEM. *P<0.05, ****P<0.0001. n=4. MDSCs, myeloid-derived suppressor cells; TNFα, tumor necrosis factor α; IFN-γ, interferon-γ.

of mMDSCs take place in primary tumors where they pave the way for tumor cell dissemination by inducing epithelial to mesenchymal transition (EMT), and higher levels of gMDSC infiltration occurs in the metastatic site where they augment the colonization and metastatic growth of disseminated tumor cells by reversing EMT (36). We observed that treatment of normal wild-type mice with MDSC exo significantly decreased the number of monocytic (m)MDSCs and increase the number of granulocytic (g)MDSCs in the spleen. As expected, we also detected a decrease in M1-macrophages in the spleen.

Tumor-associated macrophages (TAMs) are part of the heterogeneous populations of immunosuppressive myeloid cells that produce chemokines for the activation and maintenance of inflammatory processes in the TME (37-40). For the most part, M1 macrophages induce T helper type 1 cell (Th1) responses that drive cellular immunity to eliminate cancerous cells, while M2 macrophages incite Th2 responses associated with the anti-inflammatory and immunosuppressive TME, which promotes tumor growth (17,41). We observed a substantial decline of M1-macrophages and an expansion of M2 macrophages following treatment with MDSC exo that also imply their immunosuppressive effect in the TME.

We observed that MDSC-derived exosomes are able to deplete CD8+ T-cells *in vivo* and inhibit the proliferation of CD8+ T-cells *in vitro*. When activated through their antigen-specific T-cell receptor (TCR) and CD28 co-receptor, resting mature T lymphocytes start to proliferate followed by the so-called activation-induced cell death (AICD), which mechanistically is triggered by the death receptor and leads to apoptosis. The apoptotic pathway is triggered by signals originating from cell-surface death receptors that are activated by several ligands such as CD95L (FasL), tumor necrosis factor (TNF), or TNF-related apoptosis-inducing ligand (TRAIL) (42). Our protein array data demonstrated that MDSC exo contain a high level of Fas and TNF-1α, which indicate a potential role of these exosomes in inciting apoptotic pathways. We noted that MDSC exo treatment increased the activation markers of CD8+ T cells (CD69 and CD44), as well as their exhaustion marker CD279/PD-1. CD8+ T-cells also kill target cells by a cytokine-mediated mechanisms (e.g., by IFN-γ, TNF-α), which are produced and secreted as long as TCR stimulation continues. IFN-γ induces transcriptional activation of the MHC class I antigen presentation pathway and Fas in target cells, leading to enhanced Fas-mediated target-cell lysis (43). We noted that MDSC exo can activate CD8+ T cells and prompt them to generate more IFN-γ. Interestingly, ROS can control the fate of antigen-specific T cells through reciprocal modulation of the main effector

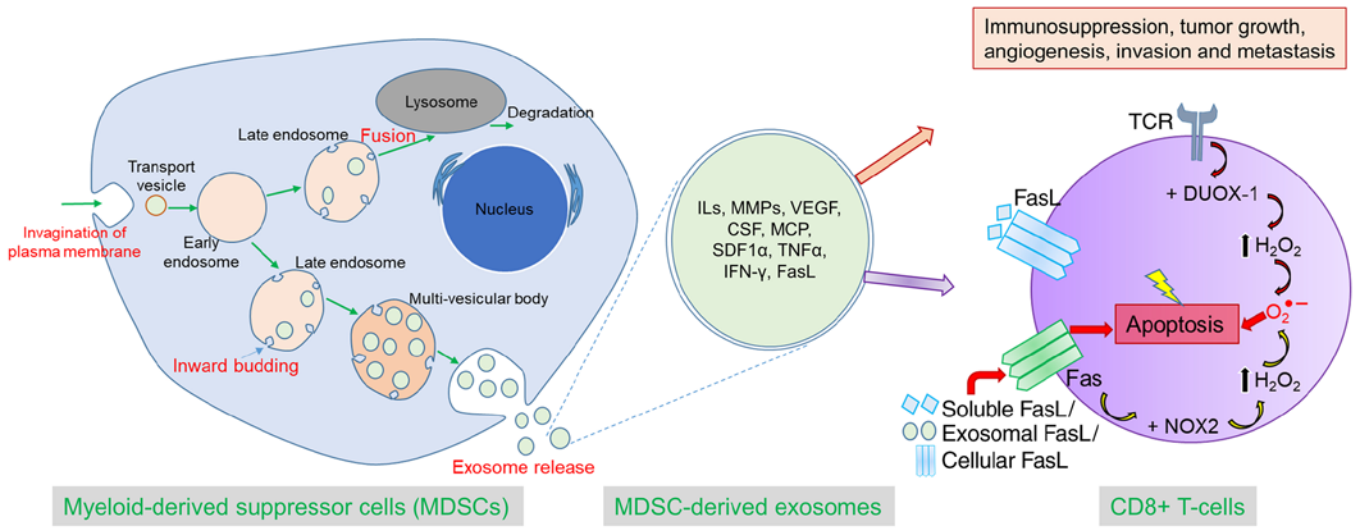

Figure 8. Schematic diagram showing the process of biogenesis of exosomes from MDSCs and the role of MDSC-derived exosomes in tumor progression and immunosuppression by AICD. Exosomes secreted from the MDSCs contain pro-tumorigenic factors from the parent cells and can play a crucial role in immunosuppression, tumor growth, angiogenesis, invasion, and metastasis by dispensing their contents into the other TME cells or distant cells. MDSC-derived exosomes can activate $CD8^+$ T-cells, and TCR triggering causes activation of DUOX-1 that leads to H_2O_2 production and eventually generation of ROS in mitochondria. Prolonged TCR stimulation triggers overexpression of both Fas (receptor) and FasL (ligand), which culminates in fratricide (from direct cell contact) or autocrine suicide (interaction of soluble FasL with Fas).

molecules FasL and Bcl-2 (44). We detected a significantly large amount of ROS production from the $CD8^+$ T-cells that were treated with MDSC exo. Therefore, we hypothesized that MDSC exo precipitate $CD8^+$ T-cell apoptosis by AICD through hyper-activation or repeated stimulation, which in turn results in increased levels of ROS production and activation of the Fas/FasL (CD95/CD95L) pathway. According to our data, we believe that ROS are involved in the reduction of $CD8^+$ T-cells and there is a possibility that ROS inhibition such as treatment with N-acetylcysteine might prevent this reduction. Although we did not look into the lymph node T-cell distribution, it will be interesting to see cellular distribution changes following MDSC exo treatment in future studies.

In summary, we comprehensively demonstrated that MDSC-derived exosomes inherit pro-tumorigenic factors and functionally resemble parental cells in immunosuppression, tumor growth, angiogenesis, invasion, and metastasis. In addition, MDSC-derived exosomes are capable of increasing ROS production and inciting the Fas/FasL pathway in $CD8^+$ T-cells, which precipitates AICD (Fig. 8). This novel concept would open up a new avenue of MDSC research and MDSC-targeted therapy.

Acknowledgements

The authors thank Dr Rhea-Beth Markowitz, Director, Office of Grant Development, Georgia Cancer Center for help with the English language editing of the manuscript.

Funding

This study was supported by the Georgia Cancer Center Startup Fund and Intramural Grant Program at Augusta University (Augusta, GA, USA) to ASA.

Availability of data and materials

The datasets used during the present study are available from the corresponding author upon reasonable request.

Authors' contributions

MHR conceived the hypothesis, designed and performed the experiments, and conducted the data collection, data analysis, and interpretation, and wrote the manuscript. TFB conducted acquisition of the *in vitro* data and edited the manuscript. RA performed the animal experiments and treated the animals. RP conducted the data interpretation and edited the manuscript. BRA helped with planning the *in vitro* T-cell experiments. HK guided MDSC collection and types, and helped with implantation of breast cancers. YL provided laboratory facilities for NTA, data interpretation, and editing of the manuscript. ASA supervised the findings of this work, aided in interpreting the results, and provided the funds and critical revision of the manuscript.

Ethics approval and consent to participate

All experiments were performed according to the National Institutes of Health (NIH) guidelines and regulations. The Institutional Animal Care and Use Committee (IACUC) of Augusta University (Augusta, GA, USA) (protocol #2014-0625) approved the experimental procedures.

Patient consent for publication

Not applicable.

Competing interests

The authors have declared that no competing interest exists.

References

1. Balkwill FR, Capasso M and Hagemann T: The tumor microenvironment at a glance. J Cell Sci 125: 5591-5596, 2012.
2. Dysthe M and Parihar R: Myeloid-derived suppressor cells in the tumor microenvironment. In: Tumor Microenvironment: Hematopoietic Cells-Part A. Birbrair A (ed). Springer International Publishing, Cham, pp117-140, 2020.
3. Achyut BR and Arbab AS: Myeloid derived suppressor cells: Fuel the fire. Biochem Physiol 3: e123-e123, 2014.
4. Arbab AS, Rashid MH, Angara K, Borin TF, Lin PC, Jain M and Achyut BR: Major challenges and potential microenvironment-targeted therapies in glioblastoma. Int J Mol Sci 18: 2732, 2017.
5. Safarzadeh E, Hashemzadeh S, Duijf PHG, Mansoori B, Khaze V, Mohammadi A, Kazemi T, Yousefi M, Asadi M, Mohammadi H, *et al*: Circulating myeloid-derived suppressor cells: An independent prognostic factor in patients with breast cancer. J Cell Physiol 234: 3515-3525, 2019.
6. Trac, N.T. and E.J. Chung: Peptide-based targeting of immunosuppressive cells in cancer. Bioactive Materials 5: 92-101, 2020.
7. Lechner MG, Liebertz DJ and Epstein AL: Characterization of cytokine-induced myeloid-derived suppressor cells from normal human peripheral blood mononuclear cells. J Immunol 185: 2273-2284, 2010.
8. Bronte V, Brandau S, Chen SH, Colombo MP, Frey AB, Greten TF, Mandruzzato S, Murray PJ, Ochoa A, Ostrand-Rosenberg S, *et al*: Recommendations for myeloid-derived suppressor cell nomenclature and characterization standards. Nat Commun 7: 12150, 2016.
9. Yang Z, Guo J, Weng L, Tang W, Jin S and Ma W: Myeloid-derived suppressor cells-new and exciting players in lung cancer. J Hematol Oncol 13: 10, 2020.
10. Corzo CA, Cotter MJ, Cheng P, Cheng F, Kusmartsev S, Sotomayor E, Padhya T, McCaffrey TV, McCaffrey JC and Gabrilovich DI: Mechanism regulating reactive oxygen species in tumor-induced myeloid-derived suppressor cells. J Immunol 182: 5693-5701, 2009.
11. Bruno A, Mortara L, Baci D, Noonan DM and Albini A: Myeloid derived suppressor cells interactions with natural killer cells and pro-angiogenic activities: Roles in tumor progression. Front Immunol 10: 771, 2019.
12. Dai J, El Gazzar M, Li GY, Moorman JP and Yao ZQ: Myeloid-derived suppressor cells: Paradoxical roles in infection and immunity. J Innate Immun 7: 116-126, 2015.
13. Geiger R, Rieckmann JC, Wolf T, Basso C, Feng Y, Fuhrer T, Kogadeeva M, Picotti P, Meissner F, Mann M, *et al*: L-arginine modulates T cell metabolism and enhances survival and anti-tumor activity. Cell 167: 829-842.e13, 2016.
14. Sinha P, Clements VK, Bunt SK, Albelda SM and Ostrand-Rosenberg S: Cross-talk between myeloid-derived suppressor cells and macrophages subverts tumor immunity toward a type 2 response. J Immunol 179: 977-983, 2007.
15. Ostrand-Rosenberg S and Fenselau C: Myeloid-derived suppressor cells: Immune-suppressive cells that impair antitumor immunity and are sculpted by their environment. J Immunol 200: 422-431, 2018.
16. Rashid MH, Borin TF, Ara R, Angara K, Cai J, Achyut BR, Liu Y and Arbab AS: Differential in vivo biodistribution of ^{131}I-labeled exosomes from diverse cellular origins and its implication for theranostic application. Nanomedicine 21: 102072, 2019.
17. Rashid MH, Borin TF, Ara R, Alptekin A, Liu Y and Arbab AS: Generation of novel diagnostic and therapeutic exosomes to detect and deplete protumorigenic M2 macrophages. Adv Ther (Weinh) 3: 1900209, 2020.
18. Du R, Lu KV, Petritsch C, Liu P, Ganss R, Passegué E, Song H, Vandenberg S, Johnson RS, Werb Z and Bergers G: HIF1alpha induces the recruitment of bone marrow-derived vascular modulatory cells to regulate tumor angiogenesis and invasion. Cancer Cell 13: 206-220, 2008.
19. Hiratsuka S, Watanabe A, Aburatani H and Maru Y: Tumour-mediated upregulation of chemoattractants and recruitment of myeloid cells predetermines lung metastasis. Nat Cell Biol 8: 1369-1375, 2006.
20. Pawelek JM and Chakraborty AK: Fusion of tumour cells with bone marrow-derived cells: A unifying explanation for metastasis. Nat Rev Cancer 8: 377-386, 2008.
21. Umansky V, Blattner C, Gebhardt C and Utikal J: The role of myeloid-derived suppressor cells (MDSC) in cancer progression. Vaccines (Basel) 4: 36, 2016.
22. Yang L, Huang J, Ren X, Gorska AE, Chytil A, Aakre M, Carbone DP, Matrisian LM, Richmond A, Lin PC and Moses HL: Abrogation of TGF beta signaling in mammary carcinomas recruits Gr-1+CD11b+ myeloid cells that promote metastasis. Cancer Cell 13: 23-35, 2008.
23. Pollard JW: Tumour-educated macrophages promote tumour progression and metastasis. Nat Rev Cancer 4: 71-78, 2004.
24. De Palma M, Venneri MA, Galli R, Sergi Sergi L, Politi LS, Sampaolesi M and Naldini L: Tie2 identifies a hematopoietic lineage of proangiogenic monocytes required for tumor vessel formation and a mesenchymal population of pericyte progenitors. Cancer Cell 8: 211-226, 2005.
25. Conejo-Garcia JR, Buckanovich RJ, Benencia F, Courreges MC, Rubin SC, Carroll RG and Coukos G: Vascular leukocytes contribute to tumor vascularization. Blood 105: 679-681, 2005.
26. Nozawa H, Chiu C and Hanahan D: Infiltrating neutrophils mediate the initial angiogenic switch in a mouse model of multistage carcinogenesis. Proc Natl Acad Sci USA 103: 12493-12498, 2006.
27. Ohl K and Tenbrock K: Reactive oxygen species as regulators of MDSC-mediated immune suppression. Front Immunol 9: 2499, 2018.
28. Ma J, Xu H and Wang S: Immunosuppressive role of myeloid-derived suppressor cells and therapeutic targeting in lung cancer. J Immunol Res 2018: 6319649, 2018.
29. De Maio A: Extracellular heat shock proteins, cellular export vesicles, and the stress observation system: A form of communication during injury, infection, and cell damage. It is never known how far a controversial finding will go! Dedicated to Ferruccio Ritossa. Cell Stress Chaperones 16: 235-249, 2011.
30. Kucharzewska P and Belting M: Emerging roles of extracellular vesicles in the adaptive response of tumour cells to microenvironmental stress. J Extracell Vesicles 2, 2013.
31. McAndrews KM and Kalluri R: Mechanisms associated with biogenesis of exosomes in cancer. Mol Cancer 18: 52, 2019.
32. Haverkamp JM, Crist SA, Elzey BD, Cimen C and Ratliff TL: In vivo suppressive function of myeloid-derived suppressor cells is limited to the inflammatory site. Eur J Immunol 41: 749-759, 2011.
33. Zhao F, Obermann S, von Wasielewski R, Haile L, Manns MP, Korangy F and Greten TF: Increase in frequency of myeloid-derived suppressor cells in mice with spontaneous pancreatic carcinoma. Immunology 128: 141-149, 2009.
34. Sevko A and Umansky V: Myeloid-derived suppressor cells interact with tumors in terms of myelopoiesis, tumorigenesis and immunosuppression: Thick as thieves. J Cancer 4: 3-11, 2013.
35. Veglia F, Perego M and Gabrilovich D: Myeloid-derived suppressor cells coming of age. Nat Immunol 19: 108-119, 2018.
36. Ouzounova M, Lee E, Piranlioglu R, El Andaloussi A, Kolhe R, Demirci MF, Marasco D, Asm I, Chadli A, Hassan KA, *et al*: Monocytic and granulocytic myeloid derived suppressor cells differentially regulate spatiotemporal tumour plasticity during metastatic cascade. Nat Commun 8: 14979, 2017.
37. Gao F, Liang B, Reddy ST, Farias-Eisner R and Su X: Role of inflammation-associated microenvironment in tumorigenesis and metastasis. Curr Cancer Drug Targets 14: 30-45, 2014.
38. Mou W, Xu Y, Ye Y, Chen S, Li X, Gong K, Liu Y, Chen Y, Li X, Tian Y, *et al*: Expression of Sox2 in breast cancer cells promotes the recruitment of M2 macrophages to tumor microenvironment. Cancer Lett 358: 115-123, 2015.
39. Dijkgraaf EM, Heusinkveld M, Tummers B, Vogelpoel LT, Goedemans R, Jha V, Nortier JW, Welters MJ, Kroep JR and van der Burg SH: Chemotherapy alters monocyte differentiation to favor generation of cancer-supporting M2 macrophages in the tumor microenvironment. Cancer Res 73: 2480-2492, 2013.
40. Allavena P, Sica A, Solinas G, Porta C and Mantovani A: The inflammatory micro-environment in tumor progression: The role of tumor-associated macrophages. Crit Rev Oncol Hematol 66: 1-9, 2008.
41. Biswas SK And Mantovani A: Macrophage plasticity and interaction with lymphocyte subsets: Cancer as a paradigm. Nat Immunol 11: 889-896, 2010.
42. Sikora E: Activation-induced and damage-induced cell death in aging human T cells. Mech Ageing Dev 151: 85-92, 2015.
43. Andersen MH, Schrama D, Thor Straten P and Becker JC: Cytotoxic T Cells. J Invest Dermatol 126: 32-41, 2006.
44. Hildeman DA, Mitchell T, Kappler J and Marrack P: T cell apoptosis and reactive oxygen species. J Clin Invest 111: 575-581, 2003.